JJMS **18**, No. 4, 665-680 (2025)

Jordan Journal of Mathematics and Statistics.
Yarmouk University

DOI:https://doi.org/10.47013/18.4.13

Effects of Relaxation times and Inclined Angles on a Material with Corrugation under Magneto-Thermal Stress

Augustine Igwebuike Anya[1,*], *Hajra Kaneez*[2], *Nnaemeka Stanley Aguegboh*[3], *Monalisa Chizoma Dike*[4]

[1,3]Department of Mathematical Sciences, Faculty of Natural and Applied Sciences, Veritas University Abuja, Bwari-Abuja, Nigeria
[2]Joint Doctoral School, Silesian University of Technology, Akademicka 2A, 44-100 Gliwice, Poland
[2]Department of Production Engineering, Faculty of Organisation and Management, Silesian University of Technology, Akademicka 2A, 44-100 Gliwice, Poland
[4]Department of Data and Information Systems, Osiri University, Lincoln, Nebraska, USA

Received: Oct. 16,2024 Accepted : July 21, 2025

Abstract: The current research deals with the Mathematical solutions for the thermo-mechanical response of surface waves on a half-space with an inclined mechanical load on the corrugated-impedance surface influenced by magnetic field and thermal stress. We utilized the harmonic approach for wave analysis in determining the solution of the model. Using Green and Lindsay theory of thermoelasticity, the distribution fields of the system such as the thermal, normal and shear stresses, and the displacement components were analytically derived. Also, the behavior of the two times relaxation constants, special angles of various inclinations and the effect of magnetism, etc., on the distributions are graphically presented using MATHEMATICA 11 software. Our computational results show that an increase in the inclined angles (special and non-special angles) produces a corresponding increase in the distribution profiles of the surface wave. Also, increase in one of the thermal relaxation constants exhibited decreasing effects on the distribution profiles whilst the temperature profile increases in modulation. Thus, our result holds true for the thermal assumptions of the temperature distribution under the considered thermo-elasticity model. Also, researchers working in the area of non-destructive material testing and evaluation would find this investigation useful; owing to the grooved-impedance coloration of the material surface and the model in its entirety.

Keywords: Relaxation times, impedance boundary, special angle of inclination, grooved boundary, magneto-thermal effects.

2010 Mathematics Subject Classification. 26A25; 26A35.

1 Introduction

The field of wave phenomena in solids is an ever old and still evolving field in solid mechanics especially as it concerned with mathematics of waves in and on materials. These wave phenomena are utilized by old and recent devices cum technologies for various scientific purposes such as in biomechanical fields, civil and structural engineering, geophysics and geothermal engineering, amongst others, for information deciphering, decision making and futuristic inferences for practical engagements. Over the years, however, Scientist in this area of specialty have devoted good front in producing mathematical models to aid the understanding associated with phenomena of waves on materials and in particular on surfaces of materials. These Mathematical models has not fall short in giving great insights to the behaviors of materials via the utilization of fundamental laws of physics and modifications where necessary on structures cum composites. Composite materials classed in the category of anisotropic materials such as the fibre-reinforced composite as posited by Spencer[1], have good tensile strength, light weight and flexible mechanical properties and thus, giving them a robust importance to the industries such as in Engineering, Architectural, Biomedical devices and material design industries. However, in enumerating the propagation of surface waves on these composite materials, a theoretical model in mathematical form are formulated while incorporating some fundamental physical effects of magnetic fields, Abd-Alla et al. [3], rotation of the medium, Schoenberg et al. [2], etc. A magnetic field tend to result in a pull or push of the material

* Corresponding author e-mail: anyaa@veritas.edu.ng, anyaaugustineigwebuike@gmail.com

depending on the model and its exhibitions since it's a vector field that prescribes the magnetic influences on moving charges and magnetic materials.

Be that as it may, impedance boundary conditions Singh [6], prescribes linear combination of unknown relations and their rate of change or gradient on a given boundary of material. They are usually utilized in many fields of physics and engineering and in particular during non-destructive testing or evaluation of materials. In addition, it is also a known theory that boundary of some materials could be in grooved or corrugated, plane or of various configurations in practice. Corrugated boundaries are seen as series of ridges or furrows that makes a difference across interfaces and results to a change in physics of the modeled problem during mechanical interactions and wave phenomena, Asano [4]. These could be represented and termed as a Trigonometric Fourier series in the mathematical sense of it. Consequently, a good number of authors have posited or opined some models which cut across theories on these ideas of grooved surfaces and similar wave propagation phenomena; Singh et al [9-11], Das et al [12], Abd-Alla et al. [13], Chattopadhyay et al. [14], Roy et al. [16], Singh et al. [17], Gupta et al. [18-19] and Anya et al [20-21], as part considerations or individual case of the interacting physical quantities especially of diverse non-homogeneous characterizations of the material other than as in combined postulations and measures presented in this current examination. Also, some of these considerations and further studies adduce the fact that the propagation of waves in thermoelasticity with two delay times (thermal relaxation times) cum dual-phase-lag in practice, Chiriţă et al.[23-24], Othman et al. [25], Kumar et al. [26-28], and Abo-Dahab et al. [29], play vital roles to studying heat flux on materials. This shows that a bulk of the work as opined in the the current referenced literature as given above lies within the physical examination and mathematical modeling of wave phenomena which underscores great importance in computational and Applied Mathematics.

Pursuant to the above given literatures, the current study tend to fill the gap in positing a mathematical model and analysis that would aid the understanding of the theoretical and computational view of the dynamic response of surface waves for a given fibre-reinforced material which incorporates two term thermal relaxation times and inclined angles with corrugated-impedance boundary under magneto-thermo-elasticity theory. This entail that the Green-Lindsay theory of thermo-elasticity is employed at this instance whilst utilizing the harmonic solution approach for wave analysis in finding the analytical solution of the modeled problem. The distribution fields of the system are analytically derived and graphically presented by considering the various effects of the contributing physical quantities of relaxation times, magnetism, corrugation parameters and angles of inclinations of various degrees.

2 The Mathematical Formulations

The mathematical constitutive relations for a fibre–reinforcement, Spencer [1], magneto-thermo-elasticity fields, Abd-Alla et al. [2] and Anya [22] are presented:

$$\sigma_{ij} = \lambda\varepsilon_{kk}\delta_{ij} + 2\mu_T\varepsilon_{ij} + \alpha\big(s_k s_m \varepsilon_{km}\delta_{ij} + \varepsilon_{kk}s_i s_j\big) + 2(\mu_L-\mu_T)(s_i s_k\varepsilon_{kj} + s_j s_k\varepsilon_{ki}) + \beta(s_k s_m\varepsilon_{km}s_i s_j) - \beta_{ij}\big(1+\nu_o\tfrac{\partial}{\partial t}\big)(T-T_o) \quad (2.1)$$

$$F_j = \mu_0 H_0^2\big(e_{,1} - \varepsilon_0\mu_0\ddot{u}_1,\ e_{,2} - \varepsilon_0\mu_0\ddot{u}_2,\ 0\big) \quad (2.2)$$

In Eqs. (2.1)–(2.2), $e = \{u_{1,1} + u_{2,2}\}$ and $\varepsilon_{ij} = \frac{1}{2}(u_{i,j} + u_{j,i})$, $i, j = 1,2,3$. The quantities σ_{ij}, λ, u_i, $T - T_o$ and F_j denote the stress tensor, displacement components, temperature difference and magnetic force, respectively. Moreover, F_j gives the components (F_1, F_2, F_3) acting on the material body. These component forces are derived from Maxwell's equations, Othman et al. [25]. Also, δ_{ij} is the Kronecker delta; $\alpha, \beta, (\mu_L - \mu_T)$ are fibre-reinforced parameters. We assume $H_i = H_0\delta_{i3} + h_i$, where $h_i = -u_{k,k}\delta_{i3}$. Here μ_0 is magnetic permeability, ε_0 electric permittivity, and H_i the magnetic field; $s = (1,0,0)$ is the fibre reinforcement directions. Thermal relaxation times satisfy $\nu_o \geq \tau_o \geq 0$. If $\tau_o > 0$, Eq. (2.4) yields finite thermal signal speed; for $\nu_o = \tau_o = 0$, we recover the classical theory. Under $|T - T_o| \ll T_o$, denote $T - T_o$ by T. The conductivity tensor is κ_{ij}, c_v the specific heat, and β_{ij} the thermal moduli.

Sequel to these, balance laws with magnetic force F_j under Green–Lindsay theory are:

$$\sigma_{ij,i} + F_j = \rho\ddot{(u_j)} \quad (2.3)$$

$$\frac{\partial}{\partial x_i}\big(\kappa_{ij}\frac{\partial T}{\partial x_j}\big) = \rho c_v\big(\frac{\partial}{\partial t} + \tau_o\frac{\partial^2}{\partial t^2}\big)T + T_o\beta_{ij}\frac{\partial E_{ij}}{\partial t} \quad (2.4)$$

Assuming motion in the x_1x_2–plane, the components of Eqs. (2.3)–(2.4) reduce to:

$$B_1\,u_{1,11}+B_2\,u_{2,12}+B_4\,u_{1,22}-\beta_1\big(1+\nu_o\tfrac{\partial}{\partial t}\big)T_{,1}=\varepsilon_0\mu_0^2H_0^2\,\ddot{u}_1+\rho\,\ddot{u}_1, \tag{2.5}$$

$$B_5\,u_{2,11}+B_2\,u_{1,12}+B_6\,u_{2,22}-\beta_1\big(1+\nu_o\tfrac{\partial}{\partial t}\big)T_{,2}=\varepsilon_0\mu_0^2H_0^2\,\ddot{u}_2+\rho\,\ddot{u}_2, \tag{2.6}$$

$$K_1\,T_{,ii}=\rho\,c_v\big(\dot{T}+\tau_o\ddot{T}\big)+T_o\,\beta_1\,\dot{u}_{i,i}. \tag{2.7}$$

Introducing dimensionless quantities

$$T'=\frac{\beta_1 T}{\rho c_0^2},\quad c_0^2=\frac{B_1}{\rho},\quad \eta_0=\frac{\rho C_v}{K_1},\quad \sigma'_{ij}=\frac{\sigma_{ij}}{\rho c_0^2},\quad (x'_k,u'_k)=c_0\eta_0\,(x_k,u_k),\quad (t',\tau'_o,\nu'_o)=c_0^2\eta_0\,(t,\tau_o,\nu_o),$$

into Eqs. (2.5)–(2.7) and dropping primes gives:

$$u_{1,11}+B_{12}\,u_{2,12}+B_{13}\,u_{1,22}-\big(1+\nu_o\tfrac{\partial}{\partial t}\big)T_{,1}=\big(\eta+1\big)\ddot{u}_1, \tag{2.8}$$

$$B_{14}\,u_{2,11}+B_{12}\,u_{1,12}+B_{15}\,u_{2,22}-\big(1+\nu_o\tfrac{\partial}{\partial t}\big)T_{,2}=\big(\eta+1\big)\ddot{u}_2, \tag{2.9}$$

$$T_{,ii}=\dot{T}+\tau_o\ddot{T}+B_9\,u_{i,i}. \tag{2.10}$$

Note $B_1=\lambda+2\alpha+4\mu_L-2\mu_T+\beta+\mu_0H_0^2$, $B_2=\alpha+\lambda+\mu_L+\mu_0H_0^2$, $B_3=\mu_L$, $B_4=\mu_L$, $B_5=\lambda+2\mu_T+\mu_0H_0^2$, $(B_{12},B_{13},B_{14},B_{15})=(B_2,B_3,B_4,B_5)/B_1$, $B_9=T_o\beta_1^2/(B_1\rho c_v)$, $\eta=\varepsilon_0\mu_0^2H_0^2/\rho$.

3 Analytical Solution

In this section, we adopt the normal mode analysis also being referred to as eigenvalue analysis approach of wave solution such that the wave thermal and mechanical displacements are presented below. This is feasible because of its satisfaction in the classical wave equation. This technique gives a feasible vibration shapes and associated frequencies that a material body will be characterized.

$$\{u_j,T-T_0=\vartheta\}=\{\bar{u}_j(x_2),\bar{\vartheta}(x_2)\}e^{\omega t+ibx_1},\quad j=1,2. \tag{3.1}$$

Introducing Eq. (3.1) into Eq. (2.5-2.7), we obtain the system of equations of homogeneous ODEs below:

$$(B_{13}D^2-b^2-(1+\varepsilon_0\mu_0^2H_0^2/\rho)\omega^2)\bar{u}_1+(iB_{12}bD)\bar{u}_2+biq\bar{\vartheta}=0, \tag{3.2}$$

$$(iB_{12}bD)\bar{u}_1+(B_{15}D^2-B_{14}b^2-(1+\varepsilon_0\mu_0^2H_0^2/\rho)\omega^2)\bar{u}_2+qD\bar{\vartheta}=0, \tag{3.3}$$

$$-B_9\,bi\omega\,\bar{u}_1-B_9\,\omega D\,\bar{u}_2+(D^2-\omega-\tau_0\omega^2-b^2)\bar{\vartheta}=0. \tag{3.4}$$

Eqs (3.2-3.4) will produce the auxiliary equation below using the principle of non-trivial solution:

$$(C_{11}(D^2)^3+C_{22}(D^2)^2+C_{33}D^2+C_{44})(\bar{u}_1,\bar{u}_2,\bar{\vartheta})=0. \tag{3.5}$$

Here, C_{jj}, $j=1,2,3,4$ (C_{jj} can be found in appendix) entails the complex coefficients of the material quantities. Recall that the auxiliary Eq (3.5) could give positive real roots say $\nu_i,i=1,2,3$. This means that we have the solution below by utilizing the normal mode analysis:

$$(\bar{u}_1,\bar{u}_2,\bar{\vartheta})=\sum_{n=1}^{3}(N_n,N_{1n},N_{2n})e^{-\nu_n x_2}. \tag{3.6}$$

The coefficients N_{1n} and N_{2n} depends on the wave number b associated with the grooved-impedance boundary and the complex frequency ω of the wave. This holds true in the x_1 direction. Substituting Eq (3.6) into Eqs (3.2-3.4), we obtain:

$$N_{1n}=H_{1n}N_n, \tag{3.7}$$

$$N_{2n}=H_{2n}N_n, \tag{3.8}$$

$$H_{1n}=\frac{(B_{13}\,\nu_n^2-b^2-p)\,\nu_n-(iB_{12}b\nu_n)\,bi}{(iB_{12}b\nu_n)\,\nu_n-(B_{15}\,\nu_n^2-B_{14}b^2-p)\,bi} \tag{9}$$

$$H1 = B_9\,\omega\Big\{(iB_{12}b\nu_n)\,bi\,\nu_n + (B_{15}\,\nu_n^2 - B_{14}b^2 - p)\,b^2 - \big[(B_{13}\,\nu_n^2 - b^2 - p)\,\nu_n^2 - (iB_{12}b\nu_n)\,bi\,\nu_n\big]\Big\} \tag{10}$$

$$H_2 = \big\{\nu_n^2 - b_1\big\}\big\{(iB_{12}\,b\,\nu_n)\,\nu_n - \big(B_{15}\,\nu_n^2 - B_{14}\,b^2 - p\big)\,bi\big\} \tag{11}$$

$$H_{2n} = \frac{H1}{H2} \tag{12}$$

The constants $p, b1, q$ are given in the appendix section. Thus, the mechanical displacement components and stress distributions on the fibre- reinforced material in non-dimensionalized forms are presented below:

$$\begin{aligned}
u_1 &= N_n e^{-\nu_n x_2 + \omega t + ibx_1},\\
u_2 &= N_n H_{1n} e^{-\nu_n x_2 + \omega t + ibx_1},\\
T &= N_n H_{2n} e^{-\nu_n x_2 + \omega t + ibx_1} + T_0,
\end{aligned}$$

$$\begin{aligned}
\sigma_{11} &= \Big[ib\big(1 - \frac{\mu_0 H_0^2}{B_1}\big) - \nu_n H_{1n} B_{16} - H_{2n}(1 + \nu_o\omega)\Big] N_n e^{-\nu_n x_2 + \omega t + ibx_1},\\
\sigma_{12} &= \big[ibH_{1n}B_{31} - \nu_n B_{13}\big] N_n e^{-\nu_n x_2 + \omega t + ibx_1},\\
\sigma_{21} &= \big[ibH_{1n}B_{13} - \nu_n B_{31}\big] N_n e^{-\nu_n x_2 + \omega t + ibx_1},\\
\sigma_{22} &= \big[ibB_{16} - \nu_n H_{1n} B_{17} - H_{2n}(1 + \nu_o\omega)\big] N_n e^{-\nu_n x_2 + \omega t + ibx_1},
\end{aligned}$$

$$n = 1,2,3, \quad B_{16} = \frac{\lambda + \alpha}{B_1}, \quad B_{17} = \frac{\lambda + 2\mu_T}{B_1}, \quad B_{31} = \frac{\mu_L}{B_1}.$$

4 Boundary Conditions

We assume that the relation associated with the grooved surface of the fibre-reinforced take the form

$$x_2 = g(x_1).$$

Here, $g(x_1)$ is a periodic function which is independent of x_3. Asano [4], represented this Trigonometric Fourier series of $g(x_1)$ in the form:

$$g(x_1) = \sum_{n=1}^{\infty}\Big(g_n e^{inbx_1} + g_{-n} e^{-inbx_1}\Big), \tag{4.1}$$

g_n, g_{-n} denotes Fourier expansion coefficients respectively whereas the series expansion order is n. This entails that the grooved boundary surface can be denoted in cosine terms, i.e.

$$g(x_1) = a\cos bx_1,$$

as posited by Asano [4]. This is such that a denotes amplitude of the grooved boundary and b the wavenumber associated with corrugated boundary surface with wavelength $2\pi/b$.

Hence, the specified grooved-impedance boundary conditions with inclined mechanical loading for the modeled problem are:

The stress components w.r.t. x_2 are continuous:

$$\sigma_{22} + \bar{\sigma}_{22} - g'(x_1)\,\sigma_{21} + \omega Z_2\,u_2 = -F_1\,e^{\omega t + ibx_1}\cos\theta,$$

$$\sigma_{12} - g'(x_1)\,\sigma_{11} + \omega Z_1\,u_1 = -F_1\,e^{\omega t + ibx_1}\sin\theta, \quad \text{at } x_2 = g(x_1),\ x_1 \text{ and } t.$$

We take thermal boundary conditions as:

$$T_{,2} = F_3\, e^{\omega t + ibx_1}, \quad \text{at } x_2 = g(x_1).$$

The given inclined load and grooved-impedance boundary are conditions in both vertical and shear stresses on the material in conjunction with the thermal conditions such that F_1 connotes the inclined mechanical loading quantity with angle θ of inclination. While F_3 denotes the thermal source parameter. Also, an additional loading $\bar{\sigma}_{22}$ due to Maxwell's stresses of electromagnetism Abd–Alla et al [2] and Anya et al [21–22] is applied. $Z_i,\ i = 1,2$ are parameters of the impedance boundary.

On Application of the boundary conditions, the results are presented for $n = 1,2,3$ as:

$$\Big\{ibB_{16} - \nu_n H_{1n} B_{17} - H_{2n}(1+\nu_o\omega) + ab\sin(bx_1)\big(ibB_{13}H_{1n} - \nu_n B_{31}\big) + \big(\omega H_{1n} Z_2 + \mu_0 H_0^2(ib - \nu_n H_{1n})\big)\Big\} N_n e^{-\nu_n g(x_1)} = -F_1\cos\theta \tag{4.2}$$

$$\Big\{(ibH_{1n} - \nu_n)B^*_{13} + ab\sin(bx_1)\Big[ib\left(1 - \frac{\mu_0 H_0^2}{B_1}\right) - \nu_n H_{1n} B_{16} - H_{2n}(1+\nu_o\omega)\Big] + \omega Z_1\Big\} \times N_n e^{-\nu_n g(x_1)} = -F_1\sin\theta \tag{4.3}$$

$$(-\nu_n H_{2n})\, N_n e^{-\nu_n g(x_1)} = F_3 \tag{4.4}$$

Hence, solving for N_n, $n = 1,2,3$ simultaneously in Eqs. (4.2)–(4.4) produces the analytical solutions for the field distributions of the model. Also, the Rayleigh-type surface wave can be obtained for traction-free boundary conditions only if $F_1 = F_3 = 0$, yielding results for a plane surface with impedance boundary.

5 Computational Results and Discussion

This section gives us the room to make computational solution and analysis to the derived field distributions. The analysis are made by presenting graphics depicting various effects of the contributing physical parameters of; inclined angles (special and non-special angles), magnetic fields, thermal relaxation times and grooved-impedance surface characterizations on the field distributions cum modulation of surface waves on the material. To achieve this, we have utilized the physical constants [15] and other parameters below whilst presenting them in Fig. (1-9). $\mu_T = 2.46\times10^{10}\,\mathrm{kg\,m^{-1}\,s^{-2}}$; $\mu_L = 5.66\times10^{10}\,\mathrm{kg\,m^{-1}\,s^{-2}}$; $\rho = 2660\,\mathrm{kg\,m^{-3}}$; $\lambda = 5.65\times10^{10}\,\mathrm{kg\,m^{-1}\,s^{-2}}$; $\beta = 220.9\times10^{10}\,\mathrm{kg\,m^{-1}\,s^{-2}}$; $\alpha = -1.28\times10^{10}\,\mathrm{kg\,m^{-1}\,s^{-2}}$; $\beta_1 = 220.9\times10^{10}\,\mathrm{kg\,m^{-1}\,s^{-2}}$; $\nu_0 = 0.15\,\mathrm{s}$; $\tau_0 = 0.12\,\mathrm{s}$; $\theta = 60^\circ$; $t = 0.6\,\mathrm{s}$; $b = 1.5$; $a = 0.9$; $F_1 = 0.4$; $F_3 = 0.1$; $x_1 = 1.3$; $Z_2 = 0.6$; $Z_1 = 0.5$; $T_0 = 293\,\mathrm{K}$; $C_v = 0.787\times10^3$; $K_1 = 0.0963\times10^3$; $\omega = -0.03 + i0.1\,\mathrm{rad/s}$; $H_0 = 100\,\mathrm{A/m}$;

Figure 1 shows the impact of the inclined angle θ on the stresses τ_{22}, τ_{12}, τ_{21}, the mechanical displacements u_i $(i = 1,2)$, and the thermal distribution T as functions of the x_2 coordinate in the fibre-reinforced medium. For these results, the contributing physical quantities—thermal relaxation constants ν_0, τ_0, magnetic field H_0, grooved boundary parameters a and b, and impedance Z_i $(i = 1,2)$—remain unchanged. Our observation reveals that an increase in the inclined angle produces a corresponding increase in the distribution profiles of the wave on the medium, except for the temperature profile, which shows a decreasing trend. All the distributions attain maximum values close to $x_2 = 0.1$, except for the normal displacement u_2 and the temperature T profile: u_2 reaches its maximum near $x_2 = 0.25$, while T peaks near the end of the x_2 coordinate, especially for decreasing angle. However, uniform behavior near $x_2 = 0.2$ is observed for the shear stresses and the horizontal displacement component u_1.

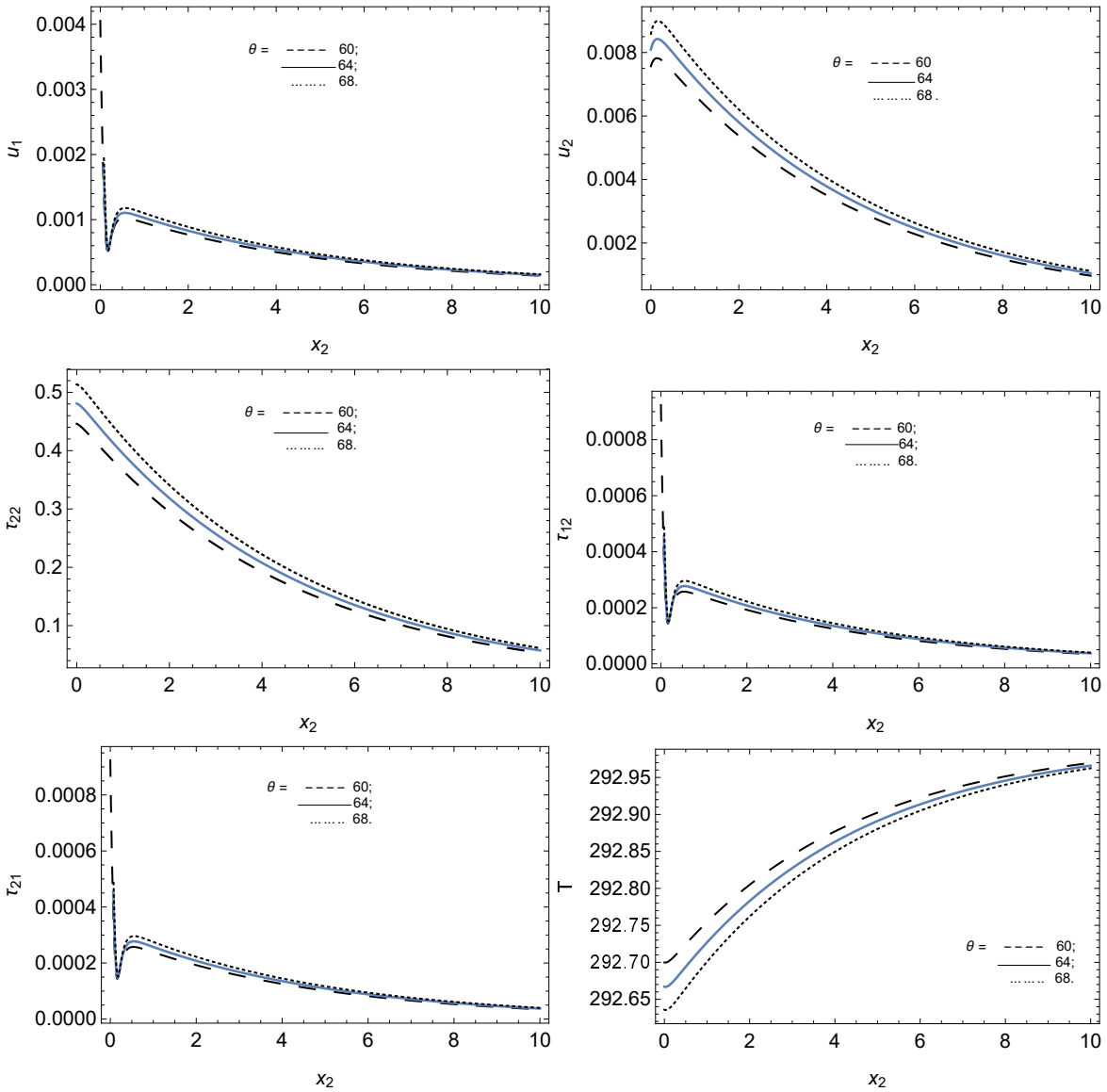

Fig. 1: Variation of inclined angle θ (degrees) on the displacement components $u_i,\ i = 1,2$, stresses τ_{22}, τ_{12}, τ_{21} and thermal distribution T versus x_2 coordinate in meters.

Furthermore, Fig. 2 demonstrates the effects of the wave number b on the stresses τ_{22}, τ_{12}, τ_{21}, mechanical displacements $u_i,\ i = 1,2$, and the thermal distribution T versus x_2 coordinate of the fibre-reinforced material, whilst the physical quantities of inclined angle θ, thermal relaxation constants v_0, τ_0, magnetic field H_0, grooved amplitude a associated with the boundary, and impedance $Z_i,\ i = 1,2$, remain fixed on the medium. We deduce from Fig. 2 that the normal distribution profile of the displacement u_2 and the temperature profile have mixed behaviors for an increase in the wave number associated with the surface, whilst obtaining their maximum near the initial and final length of the material, respectively. Also, all other distribution profiles possess increasing behavior when the value of the wave number increases. All other distribution profiles tend to yield increasing behavior when the value of the wave number is increased, whilst having maxima values similar to Fig. 1. Although, it is evident that all the distribution profiles' modulation decreases along the extended length of the material for the given change. This is due to the reinforced characteristics of the medium.

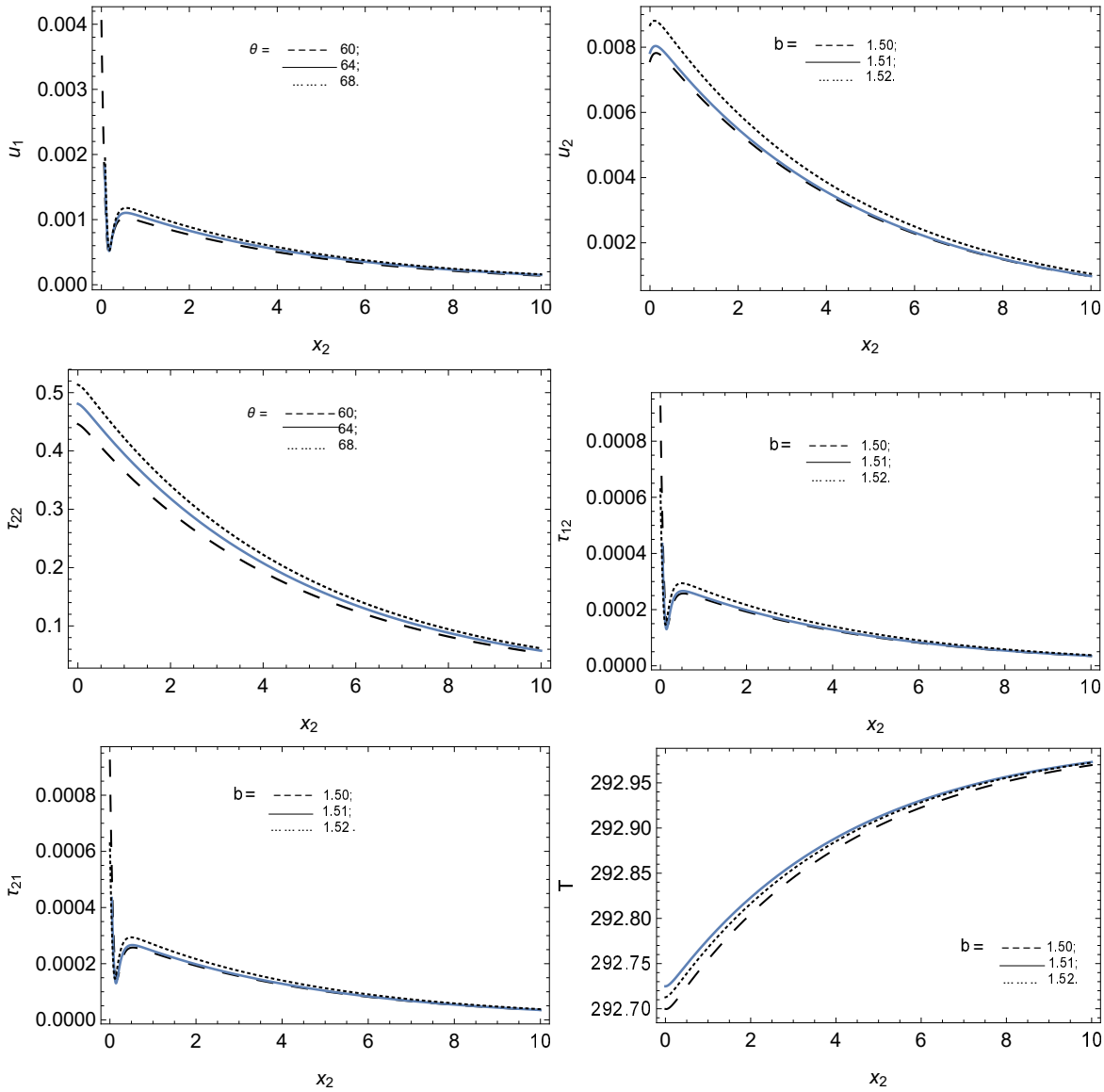

Fig. 2: Variation of wave number b on the displacement components u_i, $i = 1,2$, stresses τ_{22}, τ_{12}, τ_{21} and thermal distribution T versus x_2 coordinate in meters.

Consequently, Fig. 3 showcases the impact of the amplitude a on the stresses τ_{22}, τ_{12}, τ_{21}, displacements u_i, $i = 1,2$, and the thermal distribution T as against x_2 coordinate of the fibre-reinforced medium such that the contributing physical quantities of thermal relaxation constants ν_0, τ_0, inclined angle θ, magnetic field H_0, grooved parameter b associated with the boundary, and impedance Z_i, $i = 1,2$, are unaltered on the material. All the distribution profiles except the temperature profile demonstrate mixed behaviors for increase in the amplitude. The temperature profile T yielded an increase in modulation at this instance of increase in the amplitude a. It shows a clear sequential behavior at this increase and as compared with other distribution profiles. The maximum value of each distribution profile is not far-fetched from the analysis in Fig. 2.

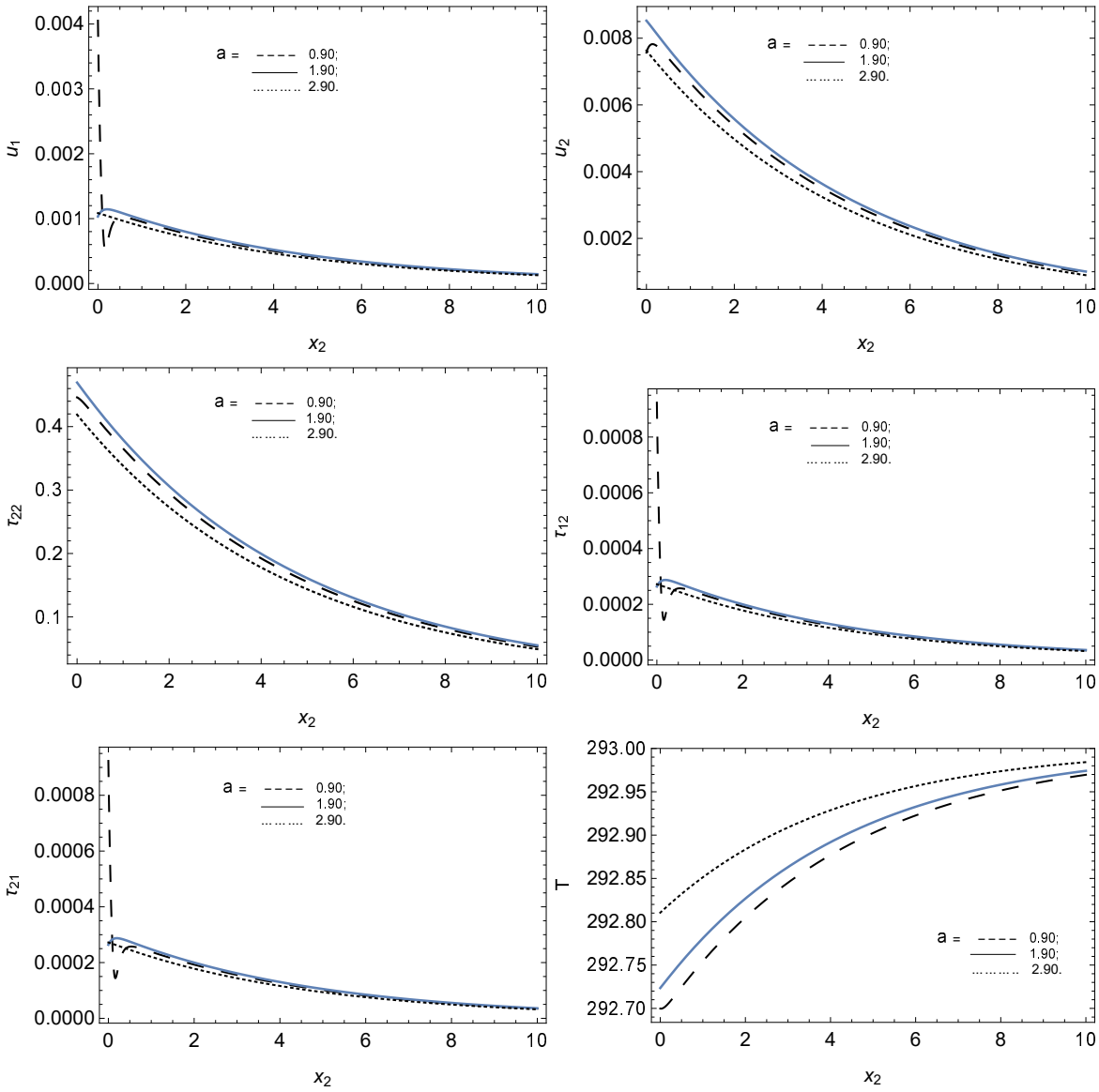

Fig. 3: Variation of amplitude a on the displacement components $u_i,\ i = 1,2$, stresses τ_{22}, τ_{12}, τ_{21} and thermal distribution T versus x_2 coordinate in meters.

Subsequently, Fig. 4 stipulates effects of the relaxation constant ν_0 on the thermal distribution T, stresses τ_{22}, τ_{12}, τ_{21}, and displacements $u_i,\ i = 1,2$, versus x_2 coordinate of the fibre-reinforced medium, following the fact that the contributing physical quantities of inclined angle θ, relaxation constant τ_0, magnetic field H_0, grooved parameters a, b and impedance $Z_i,\ i = 1,2$, are kept in a fixed manner on the fibre-reinforced medium. Owing to this, we observe that the shear stresses τ_{12}, τ_{21}, the mechanical displacements $u_i,\ i = 1,2$, and the temperature T distributions are affected in increased behaviors for increase in the thermal relaxation constant ν_0. However, the normal stress profile displays a decreasing behavior for increase in ν_0. The profiles of the shear stresses have their maximum near $x_2 = 0.2$, while the normal stress and thermal distributions have their maximum near the origin, say $x_2 = 0.09$, and near the end part of the material, say $x_2 = 9.99$, respectively. The modulations of τ_{22} and T are sequentially defined in behavior.

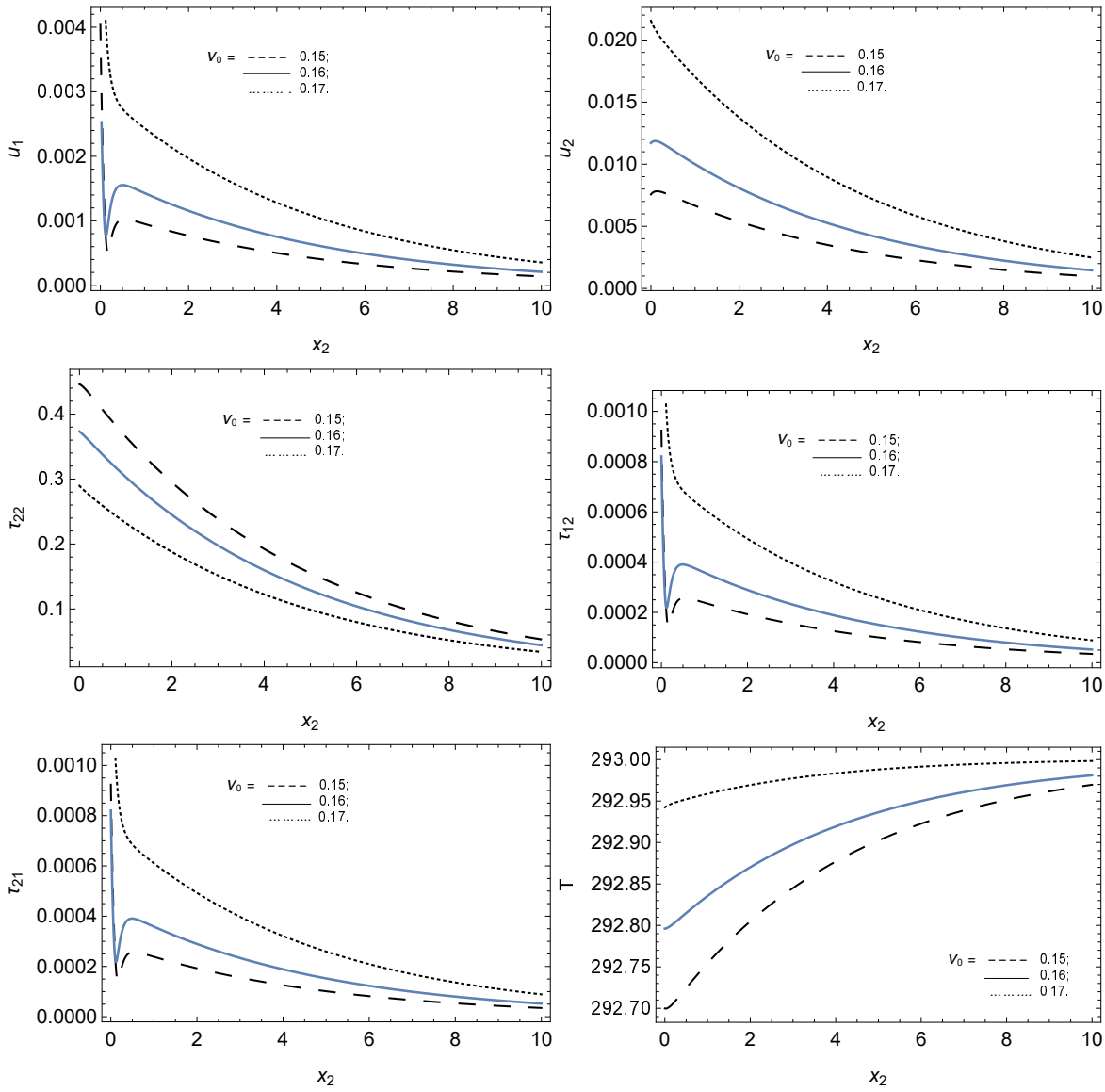

Fig. 4: Variation of thermal relaxation constant v_0 on the displacement components $u_i,\ i = 1,2$, stresses τ_{22}, τ_{12}, τ_{21} and thermal distribution T versus x_2 coordinate in meters.

In addition, Fig. 5 gives the impact of the relaxation constant τ_0 on the thermal distribution T, stresses τ_{22}, τ_{12}, τ_{21}, and displacements $u_i,\ i = 1,2$, as against x_2 coordinate of the fibre-reinforced medium whilst having the contributing physical quantities of inclined angle θ, relaxation constant v_0, magnetic field H_0, grooved parameters a, b and impedance $Z_i,\ i = 1,2$, fixed on the medium. Thus, the thermal relaxation constant τ_0 caused a decrease to the distribution profiles when varied in an increasing manner except for the thermal profile which produces increase behaviors. Hence, this entails that the more relaxation time τ_0 is given, the more we can tell how small in distribution of the fields on material could be, and thus, the modulations of the wave on the material. All field distributions hold its maximum similar to the analysis in Fig. 4 except the temperature profile which has its maximum near $x_2 = 0.25$.

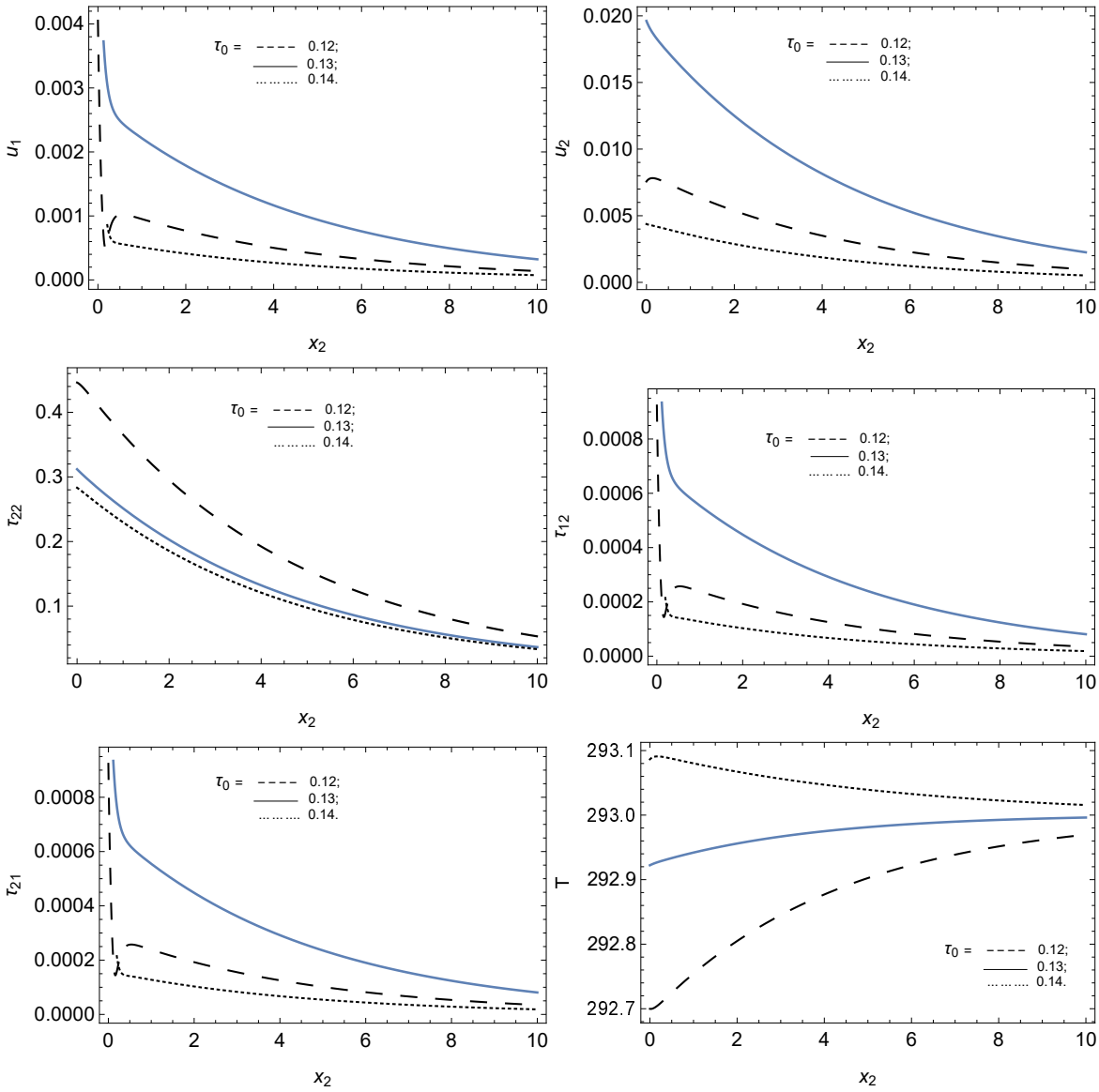

Fig. 5: Variation of thermal relaxation constant τ_0 on the displacement components $u_i,\ i = 1,2$, stresses τ_{22}, τ_{12}, τ_{21} and thermal distribution T versus x_2 coordinate in meters.

Subsequently, Fig. 6 stipulates the effect of the magnetic field H_0 on the thermal distribution T, stresses τ_{22}, τ_{12}, τ_{21}, and displacements $u_i,\ i = 1,2$, as against x_2 coordinate of the fibre-reinforced medium when the inclined angle θ, relaxation constants ν_0, τ_0, grooved parameters a, b and impedance $Z_i,\ i = 1,2$ are unarguably unchanged on the medium. The shear stresses τ_{12}, τ_{21} and the horizontal displacement u_1 profiles witnessed decrease in behaviors on the application of higher magnetic fields while temperature T and normal stress experienced mixed behaviors, i.e., in decrease cum increase exhibitions. The maximum value for the distributions could be understood from the analysis which adduces that all the profiles' maxima come close to $x_2 = 0.09$ except for the temperature profile and normal displacement components which are near $x_2 = 0.25$. Physically, both phenomena of pull and push are exhibited depending on the distribution as considered. Hence, higher application of effect of magnetism on the system would obviously yield smaller values of distribution and modulation profiles as observed, generally.

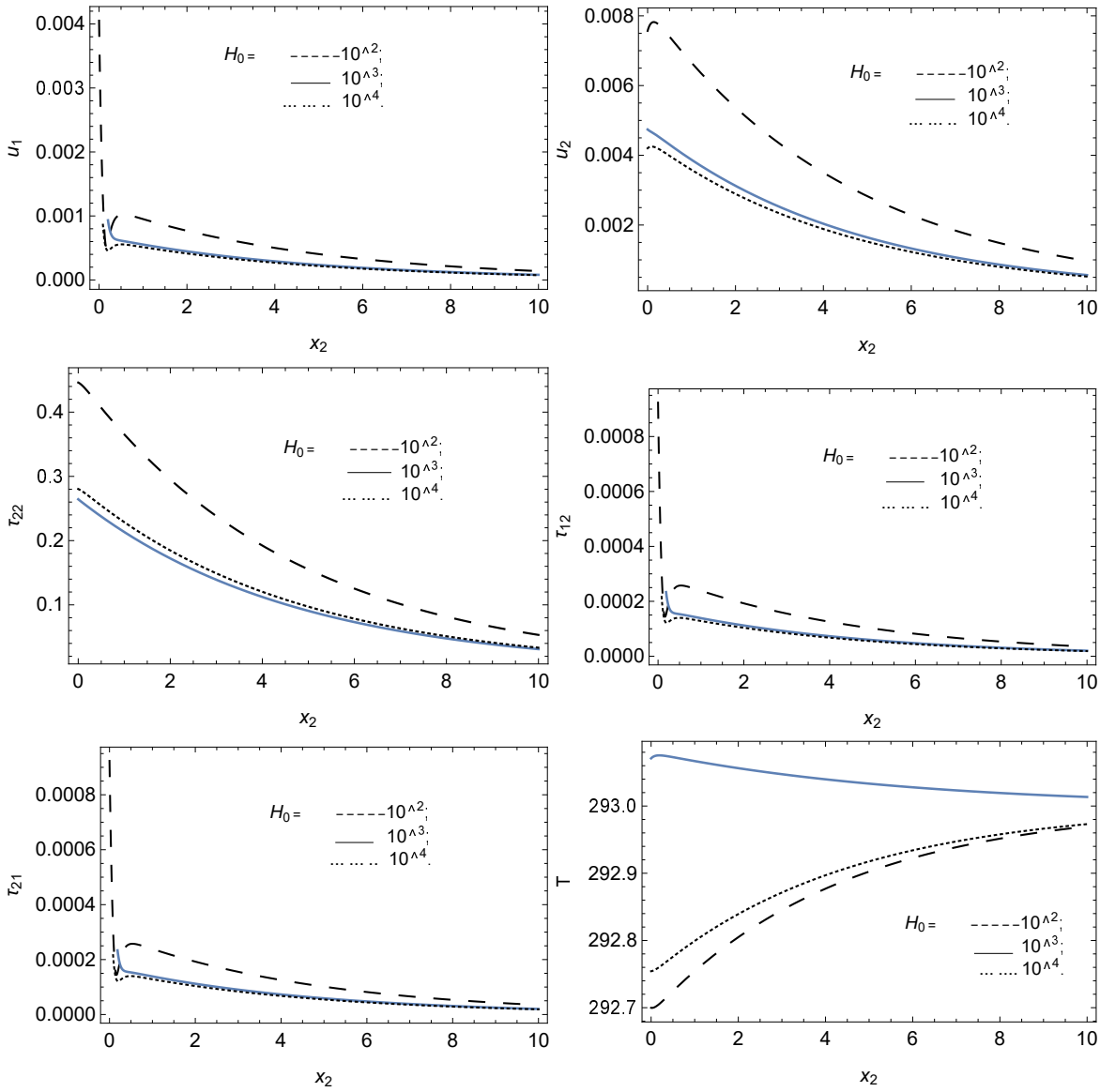

Fig. 6: Variation of magnetic field H_0 on the displacement components $u_i,\ i = 1,2$, stresses τ_{22}, τ_{12}, τ_{21} and thermal distribution T versus x_2 coordinate in meters.

Following the above, Fig. 7 demonstrate the effect of inclined special angles θ on the stresses τ_{22}, τ_{12}, τ_{21}, mechanical displacements $u_i,\ i = 1,2$, and the thermal distribution T versus x_2 coordinate of the fibre-reinforced material such that the contributing physical quantities of magnetic field H_0, thermal relaxation constants ν_0, τ_0, grooved parameters a, b associated with the boundary, and the impedance $Z_i,\ i = 1,2$, are sustained in fixed application on the material. Also, the observation we can draw from this inclined special angles is that it is similar to the analysis performed in Fig. 1. This entails that a high angle of inclination for the considered system will definitely yield corresponding high distribution profiles and modulation of the waves on the given material. However, the behavior of both figures, that is, Fig. 1 and Fig. 7 differs within the domain $0 < x_2 < 0.3$ in terms of uniform and mixed exhibitions of modulations.

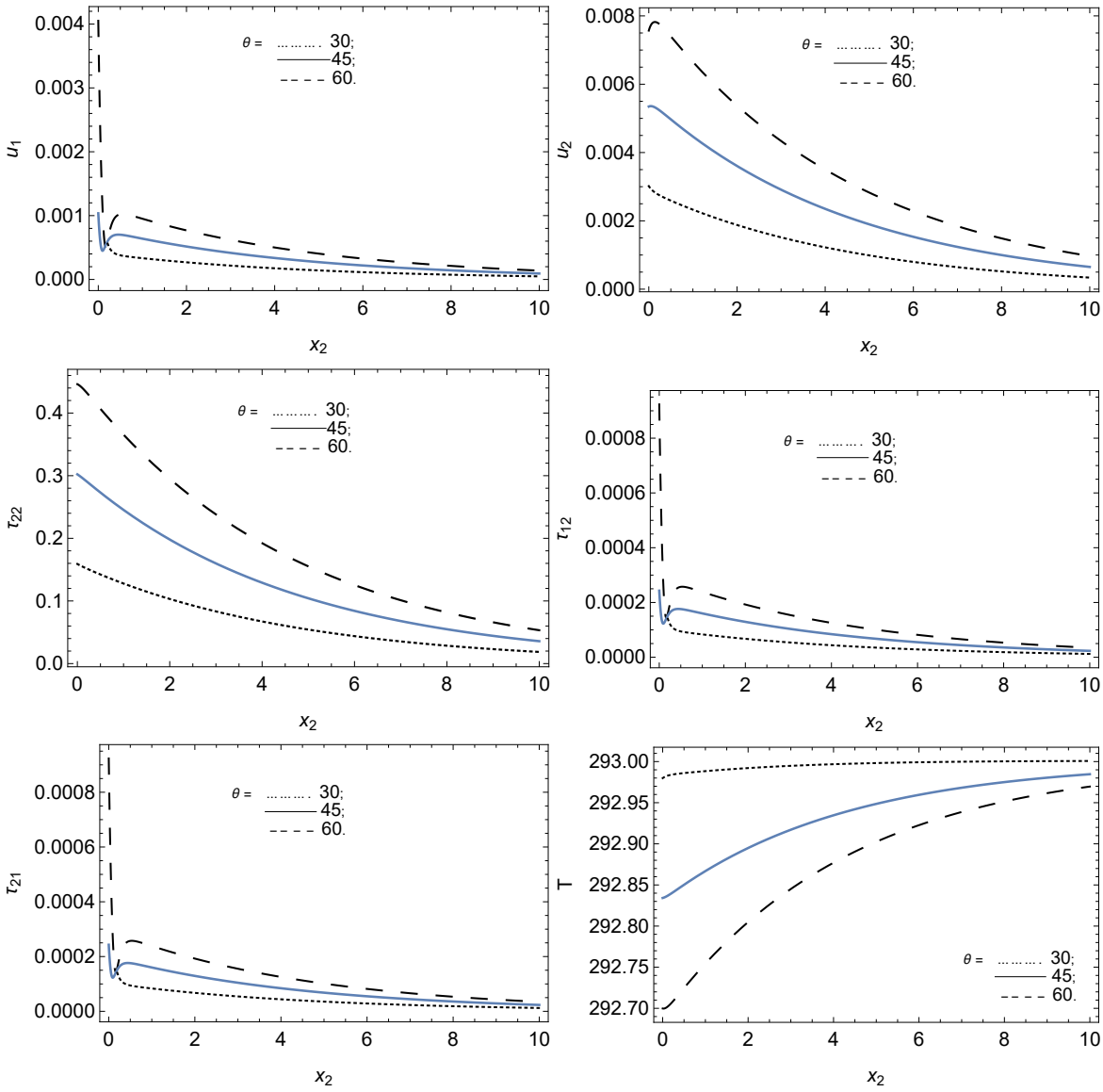

Fig. 7: Variation of inclined special angles θ (degree) on the displacement components $u_i,\ i = 1,2$, stresses τ_{22}, τ_{12}, τ_{21} and thermal distribution T versus x_2 coordinate in meters.

Nevertheless, Fig. 8 demonstrate the effect of impedance Z_2 on the stresses τ_{22}, τ_{12}, τ_{21}, mechanical displacements $u_i,\ i = 1,2$, and the thermal distribution T versus x_2 coordinate of the fibre-reinforced material. This is such that the contributing physical quantities of magnetic field H_0, thermal relaxation constants ν_0, τ_0, grooved parameters a, b, inclined angle θ associated with the boundary, and the impedance Z_1 are unchanged on the material. Fig. 8, that is, the vertical impedance Z_2 shows very negligible behavior when increased. Thus, somewhat uniform behavior is recorded in the modulation of the wave distribution profiles on the material.

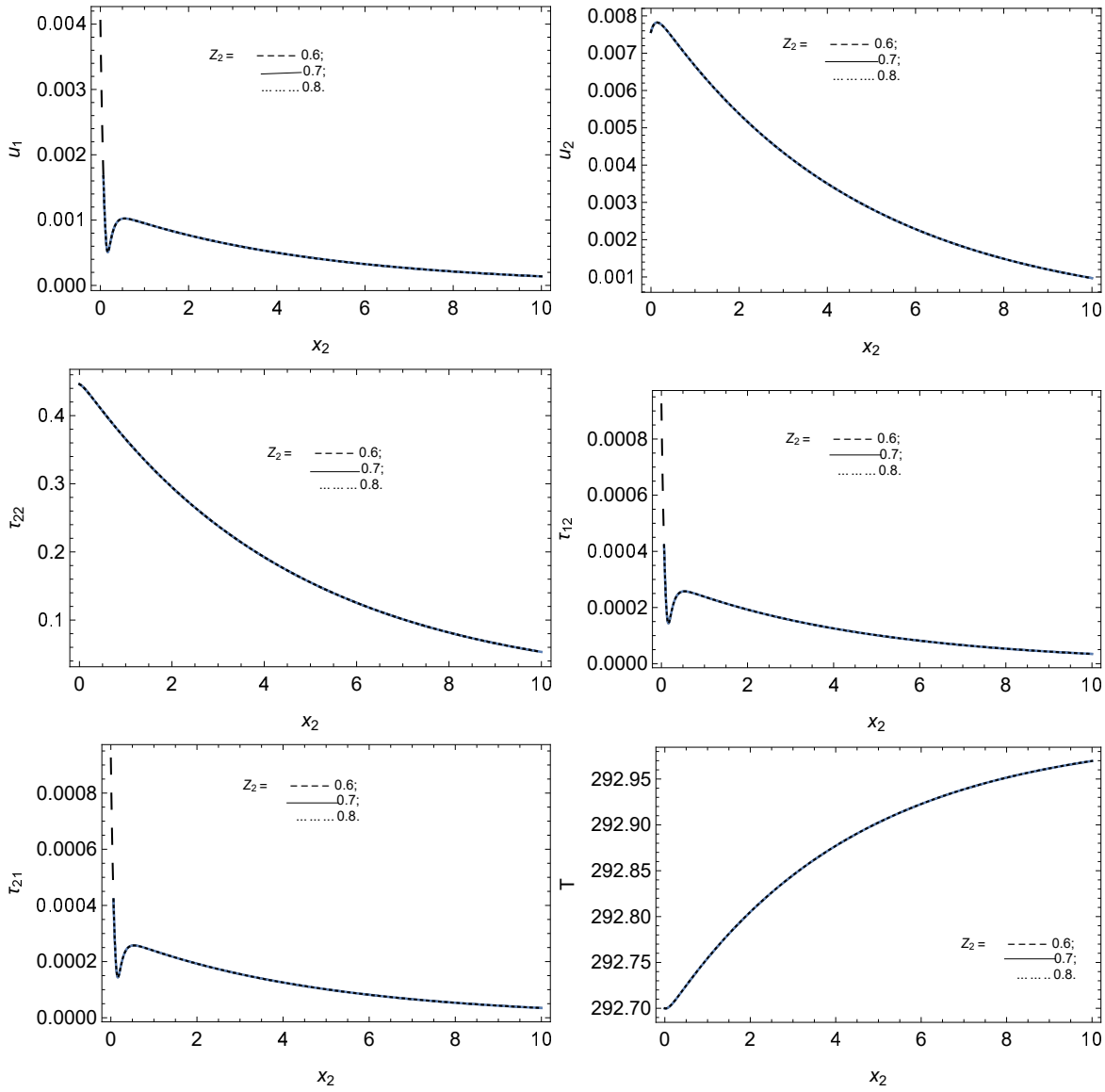

Fig. 8: Variation of impedance Z_2 on the displacement components $u_i,\ i=1,2$, stresses τ_{22}, τ_{12}, τ_{21} and thermal distribution T versus x_2 coordinate in meters.

In a similar discussion above, Fig. 9 presents the impact of the impedance Z_1 on the stresses τ_{22}, τ_{12}, τ_{21}, mechanical displacements $u_i,\ i=1,2$, and the thermal distribution T versus x_2 coordinate of the fibre-reinforced material whilst the contributing physical quantities of thermal relaxation constants v_0, τ_0, grooved parameters a, b, magnetic field H_0, inclined angle θ associated with the boundary, and the impedance Z_1 are held constant on the material. Fig. 9, i.e., the horizontal impedance Z_1 shows a very much negligible behavior as compared with the vertical impedance when increased on the material. Thus, uniform behavior is recorded in the modulation of the wave distribution profiles on the material. This entails a mechanical-like resistance towards the distribution fields and modulation of surface waves on the material.

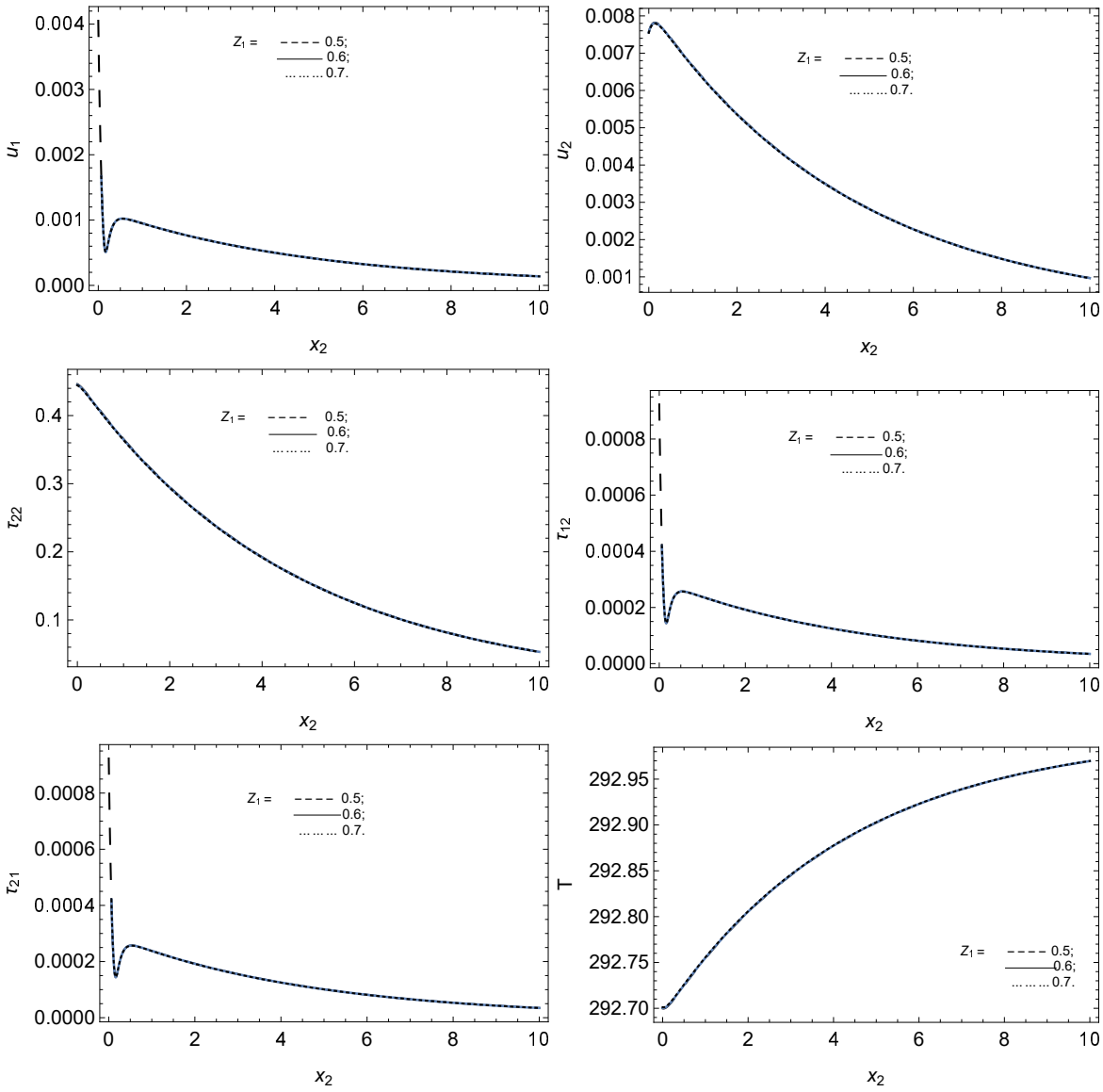

Fig. 9: Variation of impedance Z_1 on the displacement components $u_i,\ i = 1,2$, stresses τ_{22}, τ_{12}, τ_{21} and thermal distribution T versus x_2 coordinate in meters.

6 Conclusion

This study has demonstrated a concise analysis to the Mathematical solution of surface waves and the effects of thermal relaxation times constants on inclined loading of a fibre-reinforced medium with corrugated and impedance boundary surfaces under the fields of magneto-themo-elasticity. The derivations of the analytical and numerical computation were achieved via the use of the harmonic approach after the utilization of the dimensionless quantities to the dynamic equations. We observe that the effects of the contributing physical quantities to the modulation of the surface wave on the material were such that:

- –An increase in angle (special and non-special angles) of inclination for the considered system will yield corresponding high distribution profiles and modulation of the waves on the given material whilst noting some behavioral change in certain domains of the material.
- –The wave number associated with the grooved surface produced an increase in behavior to the distribution profiles on the material except for the vertical and thermal distributions which show mixed behaviors when increased.

–The amplitude associated with the grooved surface displayed a decreasing behavior to the distribution fields with some noticeable mixed behaviors to the normal displacement and normal stress distributions when increased on the material.
–The magnetic field yielded decreasing effects to the distribution profiles and thus modulation of the surface except for the thermal distribution which shows mixed behavior when increased.
–The increase in one of the thermal relaxation constants exhibited decreasing effects on the distribution profiles whilst the temperature profile increases in modulation.
–The impedance quantities showed somewhat negligible behavior to the distribution profiles, signaling a resistance-like characteristic to the modulation of the surface wave especially when increased on the material.

Hence, we conclude that this study should be able to give more insights to Scientists working in the area of wave phenomena, structural and material designers, new researchers in the field, amongst others. And aside academia, the research area is continuously being sought after in the industries like the geophysical industries in order to ascertain behaviors of vibrational media (solids or fluids) through mathematical models for proper insights, futuristic inferences and policy decision making. Also, the industrial importance of the research with respect to the Material Scientists is not far-fetched. This is such that it gives a guide in the formulation of new materials in terms of physical compositions of tensile strength, ductility, flexibility, and also with Earth Sciences associated with Atmosphere and Ocean dynamics, etc. All these information could support the UN's sustainable development goals (SDGs) in applied and computational sciences especially as it is linked to SDG 4, SDG 9, SDG 13, etc.

Declarations

Competing interests: No
Authors' contributions: Dr. Augustine Igwebuike Anya has formulated the problem, methodology, analysis, and conclusion; Dr. Hajra kaneez has prepared the manuscript, typeset, and analysis; Dr. Nnaemeka Stanley Aguegboh was instrumental to the review and discussion; and Monalisa Chizoma Dike made contributions in the area of software and the graphics.
Funding: No
Availability of data and materials: Data used are referenced and cited. They are taken from already published works of similar studies [15] and are located in the Computational and Discussion section of the manuscript.
Acknowledgments: Authors are thankful to the learned editors and referees for their valuable suggestions regarding the improvement of the paper.

References

[1] Spencer, A.J.M., *Deformations of Fibre-Reinforced Materials*, Oxford University Press, London, 1972.
[2] Abd-Alla, A.M., Abo-Dahab, S.M. and Khan, A., "Rotational effects on magneto-thermoelastic Stonely, Love, and Rayleigh waves in fibre-reinforced anisotropic general viscoelastic media of higher order", *CMC*, **53** (2017), 49–72.
[3] Schoenberg, M. and Censor, D., "Elastic waves in rotating media", *Quart. Appl. Math.*, **31** (1973), 115–125.
[4] Asano, S., "Reflection and refraction of elastic waves at a corrugated interface", *Bull. Seismol. Soc. Am.*, **56**(1) (1966), 201–221.
[5] Khan, A., Anya, A.I. and Kaneez, H., "Gravitational effects on surface waves in non-homogeneous rotating fibre-reinforced anisotropic elastic media with voids", *Int. J. Appl. Sci. Eng. Res.*, **4** (2015), 620–632.
[6] Singh, B., "Reflection of elastic waves from plane surface of a half-space with impedance boundary conditions", *Geosci. Res.*, **2**(4) (2016), 242–253.
[7] Ailawalia, P., Sachdeva, S.K. and Pathania, D., "A two dimensional fibre reinforced micropolar thermoelastic problem for a half-space subjected to mechanical force", *Theor. Appl. Mech.*, **42**(1) (2015), 11–25.
[8] Munish, S., Sharma, A. and Sharma, A., "Propagation of SH Waves in a Double Non-Homogeneous Crustal Layers of Finite Depth Lying Over a Homogeneous Half-Space", *Lat. Am. J. Solids Struct.*, **13**(14) (2016), 2628–2642.
[9] Singh, S.S. and Tomar, S.K., "qP-wave at a corrugated interface between two dissimilar pre-stressed elastic half-spaces", *J. Sound Vib.*, **317**(3) (2008), 687–708.
[10] Singh, A.K., Das, A., Kumar, S. and Chattopadhyay, A., "Influence of corrugated boundary surfaces, reinforcement, hydrostatic stress, heterogeneity and anisotropy on Love type wave propagation", *Meccanica*, **50**(12) (2015), 2977–2994.
[11] Singh, A.K., Mistri, K.C. and Mukesh, P.K., "Effect of loose bonding and corrugated boundary surface on propagation of Rayleigh-type wave", *Lat. Am. J. Solids Struct.*, **15**(1) (2018), e01.
[12] Das, S.C., Acharya, D.P. and Sengupta, D.R., "Surface waves in an inhomogeneous elastic medium under the influence of gravity", *Rev. Roum. Sci. Tech. Ser. Mec. Appl.*, **37** (1992), 539–551.

[13] Abd-Alla, A.M., Abo-Dahab, S.M. and Alotaibi, H.A., "Effect of the Rotation on a Non-Homogeneous Infinite Elastic Cylinder of Orthotropic Material with Magnetic Field", *J. Comput. Theor. Nanosci.*, **13**(7) (2016), 4476–4492.
[14] Chattopadhyay, A., "On the dispersion equation for Love wave due to irregularity in the thickness of non-homogeneous crustal layer", *Acta Geophys. Pol.*, **23** (1975), 307–317.
[15] Sunita, D., Suresh, K.S. and Kapil, K.K., "Reflection at the free surface of fibre-reinforced thermoelastic rotating medium with two temperature and phase-lag", *Appl. Math. Model.*, **65** (2019), 106–119.
[16] Roy, I., Acharya, D.P. and Acharya, S., "Propagation and reflection of plane waves in a rotating magneto-elastic fibre-reinforced semi space with surface stress", *Mech. Mech. Eng.*, **21** (2017), 1043–1061.
[17] Singh, D. and Sindhu, R., "Propagation of waves at interface between a liquid half-space and an orthotropic micropolar solid half-space", *Adv. Acoust. Vib.*, **2011** (2011), 1–5.
[18] Gupta, R.R., "Surface wave characteristics in a micropolar transversely isotropic half-space underlying an inviscid liquid layer", *Int. J. Appl. Mech. Eng.*, **19** (2014), 49–60.
[19] Gupta, R.R., "Surface wave characteristics in a micropolar transversely isotropic half-space underlying an inviscid liquid layer", *Int. J. Appl. Mech. Eng.*, **19** (2014), 49–60.
[20] Anya, A.I., Akhtar, M.W., Abo-Dahab, M.S., Kaneez, H., Khan, A. and Adnan, J., "Effects of a magnetic field and initial stress on reflection of SV-waves at a free surface with voids under gravity", *J. Mech. Behav. Mater.*, **27**(5–6) (2018), 20180002.
[21] Anya, A.I. and Khan, A., "Propagation and Reflection of magneto-elastic plane waves at the free surface of a rotating micopolar fibre-reinforced medium with voids", *J. Theor. Appl. Mech.*, **57**(4) (2019), 869–881. doi:10.15632/jtam-pl/112066
[22] Anya, A.I., "Analysis of waves subjected to mechanical force and voids source in an initially stressed magneto-elastic medium with corrugated and impedance boundary", *Scientia Iranica*, (2024), doi:10.24200/sci.2024.62816.8044
[23] Chiriţă, S. and Zampoli, V., "Wave propagation in porous thermoelasticity with two delay times", *Math. Methods Appl. Sci.*, **44** (2021), 1498–1512. https://doi.org/10.1002/mma.7869
[24] Chiriţă, S., "On the time differential dual-phase-lag thermoelastic model", *Meccanica*, **52**(1–2) (2017), 349–361. https://doi.org/10.1007/s11012-016-0414-2
[25] Othman, M.I.A. and Song, Y.Q., "Reflection of magneto-thermoelasticity waves with two relaxation times and temperature dependent elastic moduli", *Appl. Math. Model.*, **32**(4) (2008), 483–500.
[26] Kumar, R. and Ailawalia, P., "Deformations in micropolar thermoelastic medium possessing cubic symmetry due to inclined loads", *Mech. Adv. Mater. Struct.*, **15**(1) (2008), 64–76.
[27] Kumar, R. and Partap, G., "Free vibration analysis for waves in micropolar porous thermoelastic homogeneous isotropic plate with two relaxation times", *Bull. U. Politeh. Iasi*, **4** (2008), 47–74.
[28] Kumar, R., Kumar, S. and Gourla, M.G., "Deformation due to inclined loads in thermoporoelastic half-space", *J. Solid Mech.*, **8**(3) (2016), 625–644.
[29] Abo-Dahab, S.M.K., Lotfy, M.E., Gabr, M.E., et al., "Study on the effect of relaxation time and mode-I crack on the wave through the magneto-thermoelasticity medium with two temperatures", *Mech. Solids*, **58**(5) (2023), 1848–1864. https://doi.org/10.3103/S0025654423600708

Appendix

$C_{11} = B_{13}B_{15}$
$C_{22} = (-b^2i^2B_{12}^2 - (b^2+p)B_{15} - B_{13}(p - q\omega B_9 + b^2B_{14} + b1B_{15}))$
$C_{33} = (b^2p + p^2 + b^2b1i^2B_{12}^2 + b1pB_{13} + b^4B_{14} + b^2pB_{14} + b^2b1B_{13}B_{14} + b^2b1B_{15} + b1pB_{15} - q\omega B_9(b^2 + p + 2b^2i^2B_{12} - b^2i^2B_{15}))$
$C_{44} = -b^2i^2q\omega B_9(p + b^2B_{14}) - b1(b^2p + p^2 + b^2(b^2+p)B_{14})$
$p = (1 + \varepsilon_0\mu_0^2H_0^2/\rho)\omega^2$
$b1 = \omega + \tau_0\omega^2 + b^2$
$q = -(1 + \nu_o\omega)$
$B_{13}^* = \mu_L/B_1$